AGU PUBLICATIONS

JGR

Journal of Geophysical Research: Atmospheres

RESEARCH ARTICLE
10.1002/2016JD025550

Key Points:
- Anthropogenic COS inventories derived from over three-decade old data are still being used in atmospheric studies
- Updated anthropogenic COS inventories show significantly different magnitudes and spatial patterns
- Inferring process-level carbon cycle fluxes with COS requires updated anthropogenic COS fluxes

Correspondence to:
J. E. Campbell,
ecampbell3@ucmerced.edu

Citation:
Zumkehr, A., T. W. Hilton, M. Whelan, S. Smith, and J. E. Campbell (2017), Gridded anthropogenic emissions inventory and atmospheric transport of carbonyl sulfide in the U.S., *J. Geophys. Res. Atmos.*, *122*, 2169–2178, doi:10.1002/2016JD025550.

Received 20 JUN 2016
Accepted 1 FEB 2017
Accepted article online 5 FEB 2017
Published online 21 FEB 2017

Gridded anthropogenic emissions inventory and atmospheric transport of carbonyl sulfide in the U.S.

Andrew Zumkehr[1], Timothy W. Hilton[1], Mary Whelan[1], Steve Smith[2], and J. Elliott Campbell[1]

[1]Sierra Nevada Research Institute, University of California, Merced, California, USA, [2]Joint Global Change Research Institute, PNNL, College Park, Maryland, USA

Abstract Carbonyl sulfide (COS or OCS), the most abundant sulfur-containing gas in the troposphere, has recently emerged as a potentially important atmospheric tracer for the carbon cycle. Atmospheric inverse modeling studies may be able to use existing tower, airborne, and satellite observations of COS to infer information about photosynthesis. However, such analysis relies on gridded anthropogenic COS source estimates that are largely based on industry activity data from over three decades ago. Here we use updated emission factor data and industry activity data to develop a gridded inventory with a 0.1° resolution for the U.S. domain. The inventory includes the primary anthropogenic COS sources including direct emissions from the coal and aluminum industries as well as indirect sources from industrial carbon disulfide emissions. Compared to the previously published inventory, we found that the total anthropogenic source (direct and indirect) is 47% smaller. Using this new gridded inventory to drive the Sulfur Transport and Deposition Model/Weather Research and Forecasting atmospheric transport model, we found that the anthropogenic contribution to COS variation in the troposphere is small relative to the biosphere influence, which is encouraging for carbon cycle applications in this region. Additional anthropogenic sectors with highly uncertain emission factors require further field measurements.

1. Introduction

A key component of climate change modeling is characterizing the carbon-climate feedbacks driven by photosynthesis and respiration carbon fluxes [*Cox et al.,* 2000; *Friedlingstein et al.,* 2006, 2014; *Field et al.,* 2007]. Regional-scale measurements of these carbon fluxes are needed to improve the understanding of these highly uncertain feedback mechanisms. While observations of atmospheric CO_2 concentrations provide regional information on the net effect of photosynthesis and respiration surface fluxes [*Gurney et al.,* 2002], additional approaches are needed to partition the regional net flux into the photosynthesis and respiration components for a better understanding of carbon-climate feedbacks.

An emerging approach to address this critical knowledge gap is the use of atmospheric carbonyl sulfide (COS or OCS) as a regional-scale tracer of photosynthetic CO_2 uptake (gross primary production, GPP) [*Montzka et al.,* 2007; *Campbell et al.,* 2008]. Terrestrial plant uptake has been shown to be the dominant continental sink for atmospheric COS in a process that is closely related to GPP [*Campbell et al.,* 2008]. Unlike CO_2, COS does not have a large ecosystem source at regional scales. The dominant global COS source is in the tropical oceans [*Berry et al.,* 2013; *Launois et al.,* 2014; *Glatthor et al.,* 2015; *Kuai et al.,* 2015]. Because the dominant COS sink is strongly related to GPP and the dominant COS source is spatially separated from the sink, there is potential for inverse analysis of atmospheric COS observations to be used to infer regional GPP. While some canopy-scale observations have detected ecosystem COS sources at times, regional-scale evidence demonstrates that COS plant uptake dominates the variation observed in large-scale continental measurements [*Montzka et al.,* 2007; *Campbell et al.,* 2008; *Berry et al.,* 2013; *Maseyk et al.,* 2014; *Commane et al.,* 2015; *Wang et al.,* 2016; *Whelan et al.,* 2016]. Furthermore, while the relationship between plant uptake of COS and CO_2 is not constant, it is relatively stable across a range of plant species and environmental conditions [*Sandoval-Soto et al.,* 2005; *Stimler et al.,* 2010; *Hilton et al.,* 2015] and its variability exerts relatively small impact on regional-scale variations in atmospheric COS [*Hilton et al.,* 2015].

Table 1. Summary of Direct and Indirect COS Anthropogenic Sources (Gg S yr^{-1} as COS) in the U.S. From This Study and From the Kettle Inventory[a]

Source	This Study	Kettle
Rayon CS_2	0	23 ± 12
Other industry CS_2	6.1 ± 3.1	NA
Agriculture CS_2 application	5.9 ± 3.0	NA
Coal, direct COS	2.9 ± 1.2	3.6 ± 1.8
Aluminum, direct COS	1.3 ± 0.4	7.7 ± 3.9
Pigment industry		
Carbon black, direct COS	0.1–8.5	NA
Carbon black, indirect via CS_2	0.2–20.5	NA
TiO_2, direct COS	9.9 ± NA	NA
Sulfur recovery		
Direct COS	0.3–12.7	0.2 ± 0.1
Indirect via CS_2	0.1–5.5	NA
Pulp and paper		
Direct COS	15.2 ± NA	NA
Indirect via CS_2	9.9 ± NA	NA
Tires		
Direct COS	2.0 ± NA	NA
Indirect via CS_2	2.3 ± NA	NA
Total	56–103	34 ± 17

[a]NA indicates not available. Ranges for pigment and sulfur recovery assume emission sources are controlled for minimum and uncontrolled for maximum.

The use of regional COS analysis to infer GPP relies on comprehensive budgets of COS sources and sinks. Aside from the plant sink and ocean source, the most significant budget component is anthropogenic activity [*Campbell et al.,* 2015]. Previous atmospheric COS models that interpret atmospheric COS measurements rely on the gridded anthropogenic COS inventory from *Kettle et al.* [2002]. The Kettle inventory is a spatial extrapolation of a global estimate that was largely derived from industry activity data that are at least three decades old and emission factors that are known to be biased [*Campbell et al.,* 2015]. An updated gridded inventory is now needed to support COS tracer applications.

A recent inventory of anthropogenic COS sources provided an update to the global source estimate [*Campbell et al.,* 2015]. While the inventory methods from that study were used for global, historical estimates, these methods could also be applied to create spatially explicit, gridded inventories that are needed for regional COS analysis. Here we use these methods to develop a gridded inventory for U.S. emissions. The U.S. domain is of particular interest because it has the highest density of COS air-monitoring data globally which makes regional COS analysis possible in this domain [*Montzka et al.,* 2007]. We also used our new estimate of gridded anthropogenic fluxes as input to a regional atmospheric chemical transport model to explore the significance of using our revised inventory in comparison to the Kettle inventory. Our gridded 0.1° resolution inventory is available online to the scientific community at faculty.ucmerced.edu/ecampbell3/.

2. Methods

2.1. Inventory Modeling

An inventory of U.S. anthropogenic COS sources was constructed on a 0.1° resolution grid for the three dominant sectors previously considered in the Kettle inventory: direct emissions from coal combustion, direct emissions from aluminum smelting, and indirect sources from anthropogenic carbon disulfide (CS_2) emissions that are rapidly oxidized to COS in the atmosphere. We also created estimates for additional sectors that were either minor sources in the Kettle inventory or not included in the Kettle inventory. These additional sectors include the pigment industry, transportation, sulfur recovery, and the pulp and paper industry. Emissions are estimated as the product of emission factors (mass of emission per unit of anthropogenic activity) and spatially and temporally explicit U.S. industry activity data. Detailed emission factor information is provided in *Campbell et al.* [2015] which was shown to provide a significant update to the outdated emission factor data applied in the Kettle inventory. The emission factor approach from *Campbell et al.* [2015] is also summarized below along with the data we used for U.S. industry activity. The approach from the Kettle inventory is also briefly summarized below for comparison. Our results for each of the COS sources described below are summarized in Table 1.

2.1.1. Coal Combustion

The inventory for the U.S. coal COS source utilizes updated emission factors from the NASA North American Intercontinental Chemical Transport Experiment airborne campaign which revealed that the single emission factor observation used in Kettle inventory underestimated the U.S. emission factor by a factor of 2 [*Blake et al.,* 2008]. Based on these data, we used an emission factor of 2.3 and 6.0 ppt COS ppm CO_2^{-1} for the

western and eastern U.S. regions, respectively. The industry activity was based on year 2010 national coal consumption [*U.S. Energy Information Administration,* 2002]. We extrapolated this estimate in space and time using U.S. county-level coal consumption data which was available for the year 2002 [*U.S. Energy Information Administration*, 2003]. The industry activity approach for the Kettle inventory was based on the global coal consumption in year 1989 which was spatially and temporally extrapolated using year 1985, 1° gridded anthropogenic SO_2 emissions.

2.1.2. Aluminum Smelting

Aluminum emission factors have been examined for a range of anode sulfur contents, emission control devices, and smelter types (prebake and Söderberg smelters) [*Kimmerle and Noel*, 1997; *Utne et al.,* 1998]. Based on these data, we used an emission factor of 0.9 kg S t Al^{-1}. The Kettle inventory overestimated the emission factor due to a failure to account for smelter types and the nonlinear relationship between anode sulfur content and COS emissions [*Utne et al.,* 1998]. Industry activity was based on individual production levels at each aluminum smelter in the U.S. for the year 2012 [*U.S. Geological Survey*, 2013]. The industry activity approach for the Kettle inventory was based on the global aluminum production in year 1995 which was spatially and temporally extrapolated using year 1985, 1° gridded anthropogenic SO_2 emissions.

2.1.3. Industrial CS_2 Applications

Global anthropogenic COS sources are dominated by the indirect source from industrial CS_2 emissions during rayon production [*Campbell et al.,* 2015; *Lee and Brimblecombe*, 2016]. The emitted CS_2 is rapidly oxidized to COS in the troposphere [*Chin and Davis*, 1993]. Atmospheric oxidation of CS_2 to COS has a molar conversion efficiency that has been estimated at 81% [*Chin and Davis*, 1993]. In the U.S., rayon production has been in decline beginning in the 1970s and is no longer produced in the U.S. using CS_2 [*Blagoev and Funada*, 2011; *Fiber Economics Bureau*, 2014]. Thus, our inventory does not include rayon emissions. However, the Kettle inventory includes a large rayon source in the U.S. because it uses a map of 1985 anthropogenic SO_2 emissions to scale the global rayon source in space.

Atmospheric emissions of CS_2 have also been reported from other applications including solvents and agriculture chemicals [*Peyton et al.,* 1978; *Blagoev and Funada*, 2011]. To estimate emissions from these categories, we use year 2010 U.S. consumption data of 20,000 t for agriculture CS_2 application and 21,000 t for other industrial applications [*Blagoev and Funada*, 2011]. We assume that 80% of these applications are emitted to the atmosphere as CS_2 due to high volatility and low solubility in water [*Chin and Davis*, 1993]. We scale the industrial applications in space using EDGAR v4.2 fields of N_2O, and we scale the agriculture applications using a U.S. cropland map [*Joint Research Centre*, 2011; *Zumkehr and Campbell*, 2013]. We use the 81% molar conversion efficiency for this and all subsequent CS_2 emissions.

Future measurements may allow the differentiation of emission factors by crop types, management, and industrial applications. Nevertheless, our approach using U.S. specific data represents an advance over the Kettle inventory which relied on an estimate of the year 1984 consumption of rayon which was spatially and temporally extrapolated using year 1985, 1° gridded anthropogenic SO_2 emissions.

2.1.4. Additional Sources

We also estimated sources from sectors that were either minor sources in the Kettle budget or not included in that inventory. The pigment industry has been noted to emit COS and CS_2 but was not accounted for in the Kettle inventory. First, we consider the pigment carbon black which includes sources of COS and CS_2. For carbon black, emission factors are 10 kg COS/Mg carbon black produced and 30 kg CS_2/Mg carbon black produced [*Blake et al.,* 2004]. Previous work noted that the emission factors were reduced by 99% in developed countries due to emission controls [*Blake et al.,* 2004]. We used the controlled and uncontrolled emission factors to provide a lower and upper range for this source. As with all indirect emissions from CS_2, we use the molar oxidation conversion factor from CS_2 to COS of 81%. For industry activity, we use the U.S. carbon black production in year 2015 of 1.6×10^6 t. Production of the pigment TiO_2 results in direct emissions of COS. We used an emission factor of 14.7 g COS/kg of TiO_2 produced [*Blake et al.,* 2004] and industry activity of 1.26×10^6 t for the year 2014 [*Lee and Brimblecombe*, 2016].

For the tire wear source, which were not included in the Kettle inventory, we base our emission factor on the following emission data: 1.17 kg rubber emitted/car/yr, 1.6% sulfur content of rubber, and a fraction of sulfur emissions as 43% COS and 57% CS_2 [*Pos and Berresheim*, 1993; *Lee and Brimblecombe*, 2016]. The activity for the tire emissions is 253 million U.S. vehicles.

Next we estimate emissions from sulfur recovery which were a minor source in the Kettle inventory. Previous inventories have used an emission factor of 0.263 g COS/kg sulfur recovered [*Peyton et al.,* 1978]. However, more recent reports for U.S. emission factors are 0.1 and 2.7 g COS/kg sulfur recovered for controlled and uncontrolled emissions, respectively, and 0.02 and 0.9 g CS_2/kg sulfur recovered for controlled and uncontrolled emissions, respectively. Here we use the more recent estimates to provide a lower and upper limit. For industry activity, we used 9×10^6 t of sulfur recovery in the year 2014 [*Apodaca*, 2015].

The global pulp and paper industry has previously been reported to result in 97 Gg S-COS/yr and 79 Gg S-CS_2/yr [*Lee and Brimblecombe*, 2016]. Here we scale this global estimate to U.S. emissions based on the ratio of U.S. to global pulp and paper production (16%). This sector was not included in the Kettle inventory.

At present, the emission factor data are highly speculative for these additional sources. Thus, we included estimates of these sources in our national estimates for comparison with other sectors (Table 1), but we did not include these additional sources in our gridded inventory.

2.2. Atmospheric Transport Modeling

We used our gridded anthropogenic COS inventories and the Kettle inventory as input to the Sulfur Transport and Deposition Model (STEM) with meteorological fields provided by the Weather Research and Forecasting version 2.2 (WRF) model. STEM has been widely applied for analysis of anthropogenic and biosphere exchange with the atmosphere for U.S. and other regional domains [*Carmichael et al.,* 1991; *Campbell et al.,* 2007; *D'Allura et al.,* 2011; *Kulkarni et al.,* 2014]. STEM is a mesoscale, 3-D Eulerian model that employs a finite difference numerical approach to solve the chemical continuity equation. The WRF and STEM simulations were completed for July and August in year 2008 and have a 60 km horizontal resolution and 22 vertical levels. While simulations of the seasonal cycle are an important next step for future studies, the growing season focus of the present study is useful because this is the time period when the COS tracer approach is most likely to yield information on GPP due to the peak growing season conditions. For comparison, we simulated the atmospheric signature of the biosphere using plant uptake fluxes from *Hilton et al.* [2015].

3. Results

The U.S. total emissions for our estimates and the Kettle inventory are compared in Table 1. In total, U.S. anthropogenic sources of COS, from our estimate, are only 47% of the Kettle source estimate when only comparing the sources considered in the Kettle inventory. Including other sectors leads to a much larger anthropogenic source, but these sectors are based on speculative emission factors.

While the coal source of COS was found to be similar in magnitude in both estimates, the updated inventory for the aluminum source of COS is 17% of the previous estimates and the industrial CS_2 inventory is 52% of the previous estimates. The difference for aluminum is due to the recent data showing a lower emission factor, and the difference for CS_2 is largely due to the decline of the U.S. rayon industry.

The large difference in the industrial CS_2 source estimate between our inventory and the Kettle inventory is due to the fact that the Kettle inventory is based on a global, gridded SO_2 emission inventory as a proxy for spatial scaling. While SO_2 emissions may be useful as a preliminary spatial scalar of anthropogenic activity, they lead to large regional biases in COS emission estimates because industrial CS_2 activity has a very different spatial distribution than SO_2 emissions. The Kettle emissions result in a large CS_2 source in the U.S., but our industry-specific data show that CS_2 emissions in the U.S. are relatively small.

The differences between the detailed U.S. inventory in this study and the preliminary U.S. inventory from *Campbell et al.* [2015] are due to several factors. First, this study estimates a smaller coal source because of differentiation of emission factors for the eastern and western U.S. while *Campbell et al.* [2015] assumed a constant national emission factor. Second, we estimate a larger CS_2 source because we account for CS_2 use reported from multiple industrial and agriculture activities while *Campbell et al.* [2015] focused on rayon. Finally, we find a smaller aluminum source because we assume that smelters are evenly split between prebake and Söderberg smelters while *Campbell et al.* [2015] assumed that the fraction was the same as the global mix (90% of smelter are prebake).

Emission factors and industry activity data both contribute to the differences found in our estimate compared to previous work. Our coal emissions are based on a larger set of measurements that suggest an emission

factor that is double the rate assumed in the Kettle inventory [*Blake et al.,* 2008]. Furthermore, our spatial scaling is based on recent U.S. county-level coal consumption data which provides a different level of industry activity than assumed by the SO_2 scaling approach in the Kettle inventory. Although new industry activity data and emissions factors are used here, our estimate for the magnitude of the coal source remains similar to that of the Kettle inventory because the increased emissions factor offsets the smaller industry activity totals.

We also report large sources for other sectors that were either minor sources in the Kettle inventory or not included (Table 1). When considering these additional sources that are not taken into account in the Kettle inventory, our estimate becomes approximately 1.6 to 3 times larger than that of the Kettle inventory. These additional sources could be much larger than the CS_2 application, coal, and aluminum sources described above. However, these estimates are based on highly uncertain emission factor data in comparison to the emission factor data available for CS_2 application, coal, and aluminum. The upper limit for the total source of 103 Gg S yr^{-1} seems particularly unlikely given the persistent drawdown of tropospheric COS observed over North America during the growing season [*Campbell et al.,* 2008].

While the national-scale source from coal is similar for our estimate and the Kettle inventory, the spatial variation is different. Comparison of emissions maps (Figure 1, left) shows a high concentration of the coal COS source in the northeast for the Kettle inventory but a more widely dispersed source in our estimates. The surface enhancement in atmospheric COS mixing ratios in the boundary layer as simulated by STEM/WRF can exceed 10 ppt in regions of anthropogenic activity (Figure 1, right).

While the Kettle inventory uses the same spatial scaling for all anthropogenic sectors, our emissions inventory uses industry-specific data for the spatial scaling of each sector. The aluminum emissions were based on aluminum smelting data, giving the locations of individual smelting plants, and are mapped in Figure 2. The revised aluminum estimates also show a wider distribution than the Kettle emissions, particularly in the midcontinent, southeast, Texas, and northwest.

Figure 3 shows the spatial distribution of anthropogenic CS_2 sources of anthropogenic COS for industrial activity (top) and agriculture applications (bottom). While Kettle used the same spatial scaling based on SO_2 for all sources of COS (Kettle CS_2 distribution would look identical to Figure 1 (top row, left), but with a higher magnitude), our distribution based on cropland locations and industrial N_2O provide a much different spatial representation of the CS_2 sector. We find emissions of modest magnitude spread over large areas for sources derived from agriculture CS_2 applications and intense hot spots from the industrial CS_2 sector.

The wider spatial distribution in our estimates includes regions where NOAA air-monitoring sites are located (Figures 1–3) [*Montzka et al.,* 2007]. In particular, our emissions show that some NOAA sites are located within hot spots of anthropogenic COS emissions. While the plant uptake is generally thought to be much larger than the anthropogenic source [*Campbell et al.,* 2008], these revised emission estimates may be useful in reducing the uncertainty associated with interpreting COS observations at the colocated sites.

To this end, we examined the influence of anthropogenic emissions on the NOAA sites that are located within regional hot spots of anthropogenic emissions. STEM/WRF simulations that were driven by only plant uptake show a widely dispersed and large sink that is characteristic of ecosystem fluxes (Figure 4). These simulations are consistent with the large plant uptake flux in the Corn Belt region and the prevailing westerly winds that result in low tropospheric COS mixing ratios in the midcontinent region. We extracted simulated vertical profiles from three STEM/WRF runs that were driven by plant uptake, our coal emissions, and the Kettle coal emissions (Figure 5). We considered the NOAA airborne monitoring stations at HIL (Homer, Illinois, USA) and SCA (Charleston, South Carolina, USA).

Two metrics are compared at these monitoring sites: average July concentrations and the day of peak anthropogenic mixing ratio enhancement. The peak anthropogenic day is solely due to transport because there is no daily variation in our anthropogenic emission estimate. Even in these emission hot spots, the simulated biosphere signal is roughly twice the anthropogenic signal for the average monthly vertical profile (Figure 5, top row). This is due to the large spatial extent of the biosphere sink. However, for the peak anthropogenic day, the anthropogenic signal can be similar in magnitude to the biosphere signal on that same day (Figure 5, bottom row). This suggests that the climatological analysis of air-monitoring data will be less sensitive to anthropogenic emissions, but a more time-resolved analysis of these data will benefit from the improved emissions inventory presented here.

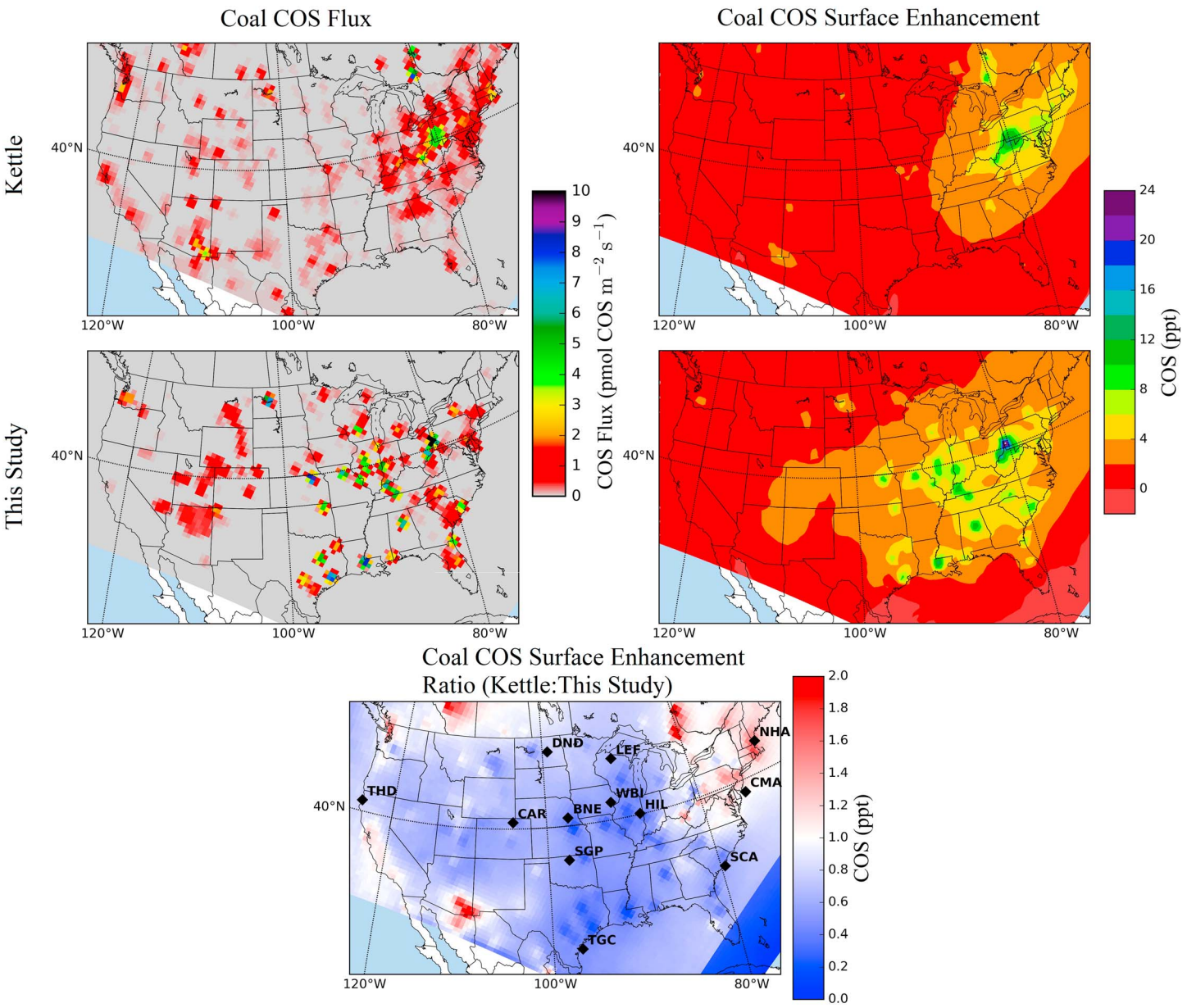

Figure 1. Comparison of coal COS sources from the Kettle inventory (top row) and our updated inventory (middle row) and the ratio of the surface enhancements from the previous COS inventory and from this study (bottom). Modeled surface enhancement is for July and August (mean difference between free troposphere and boundary layer mixing ratios).

4. Discussion

Here we have demonstrated that updated anthropogenic COS inventories based on more recent industrial activity and emissions factors data have significantly different magnitudes and spatial distributions than previous inventories that were based on a smaller subset of emission factor data and outdated industry activity data. Additionally, we demonstrated that the simulated impact on the atmosphere based on this new anthropogenic COS emissions inventory can have very different spatial signatures (including the coal sector, despite similar magnitudes) (Figure 1). It follows that interpretations of observations using these simulations could be similarly biased, especially if the study area or observation site is near anthropogenic COS hot spots.

The analysis presented here includes multiple sources of uncertainty in the emission estimates and the transport simulations. The uncertainty in the atmospheric transport simulations is a result of uncertain

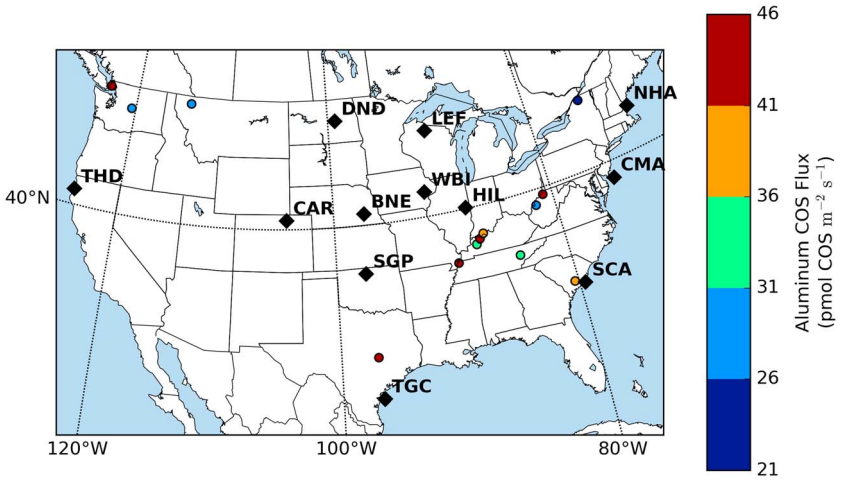

Figure 2. COS flux from aluminum smelting in the US for 2012 (circles) and locations of NOAA air-monitoring sites that measure atmospheric COS from airborne platforms in the U.S. (diamonds). Additional surface sites not shown here but are presented in *Montzka et al.* [2007].

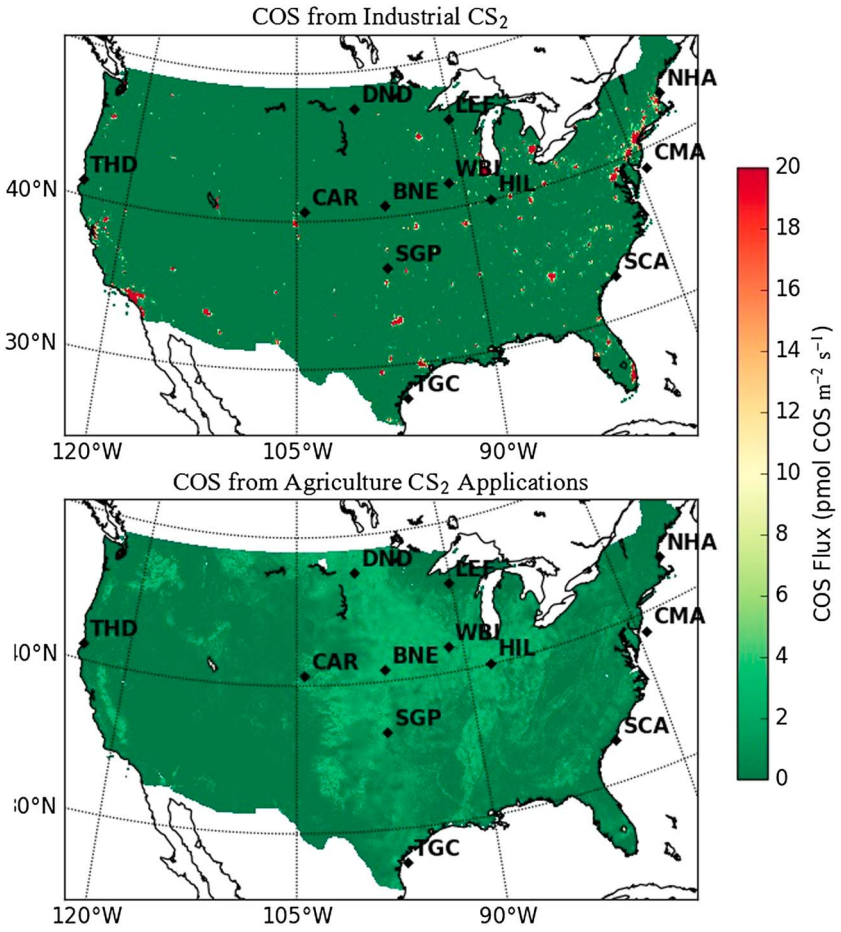

Figure 3. COS sources from anthropogenic CS_2 applications to (top) industrial processes and (bottom) agriculture CS_2 applications.

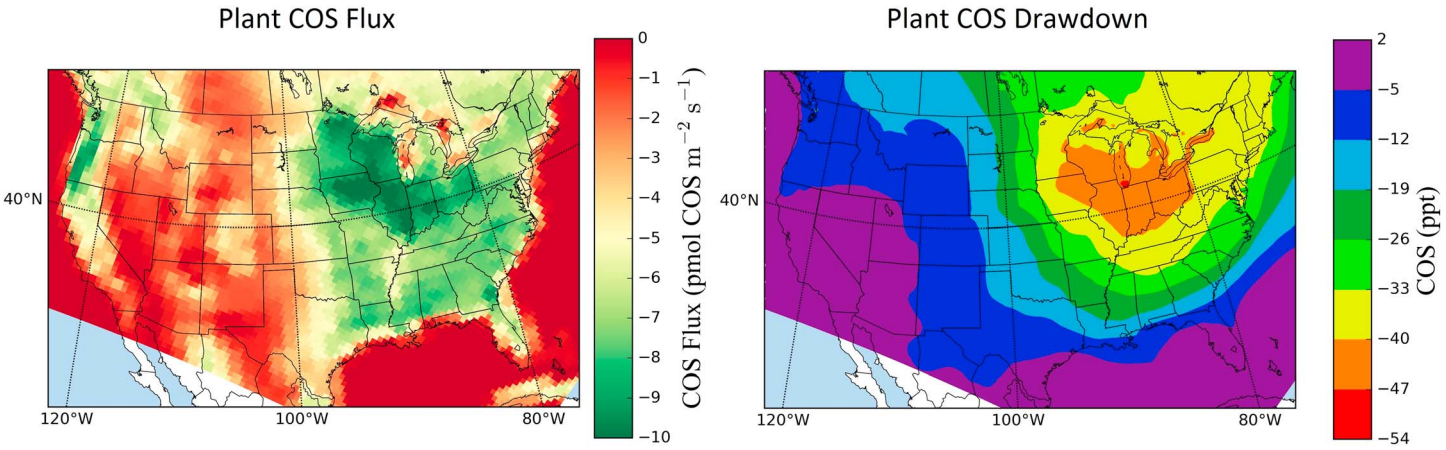

Figure 4. CASA GFED-3 (left) plant COS flux and the average (right) plant COS tropospheric vertical drawdown for July and August 2008, simulated by the STEM/WRF atmospheric transport model with CASA GFED-3 COS plant surface fluxes.

meteorological data, numerical integration, and subgrid processes. STEM model accuracy has been demonstrated in previous work [*Campbell et al.,* 2007, 2008; *D'Allura et al.,* 2011]. However, these uncertainties will have similar effects on all three transport simulations presented in this paper and should not influence our conclusions regarding the comparison of the three cases.

The main sources of uncertainty for the magnitude of the anthropogenic emissions depend largely on the emissions factors. The industry activity data, on the other hand, are likely to be more accurate due to the economic importance of tracking these data. The estimated uncertainty for the magnitudes of anthropogenic COS sources from this study are ±30% for aluminum and ±40% for coal. CS_2 uncertainty is represented here as an upper estimate due to source data limitations where the lower estimate is based on an emissions factor previously applied to a study in Japan that used an emissions factor that was half of what was used here [*Blake et al.,* 2004].

The spatial pattern of the coal COS source is based on county-level coal consumption data which is sufficient for regional analysis that is the intended application of this inventory. However, for applications that require higher resolution, the point locations of these power plants could be used to create a finer emissions grid.

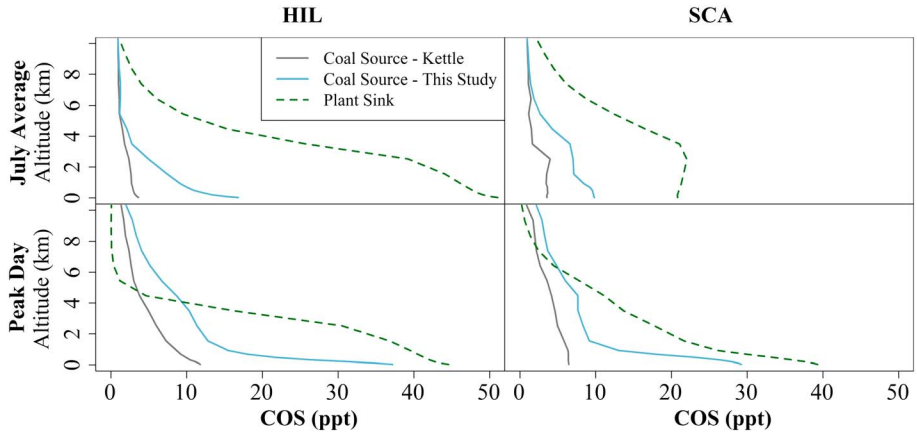

Figure 5. A comparison of the average coal COS surface enhancement from this study (blue), from the Kettle inventory (grey) and plant COS drawdown from CASA GFED-3 (dashed green line) at the Homer, Illinois (HIL), and Charleston, South Carolina (SCA), NOAA airborne monitoring sites for July and August and the peak coal COS enhancement day. The *x* axis shows the absolute value of the vertical profile (both the biosphere drawdown and anthropogenic enhancement are plotted as positive on the *x* axis) to allow for visual comparison of the biosphere and anthropogenic activity.

Aluminum emissions are more easily resolved spatially as there are relatively few smelting plants and the location and production share are known for each [*U.S. Geological Survey*, 2013].

The atmospheric transport simulations presented in this study were conducted to examine the sensitivity of atmospheric COS profiles to the industrial source relative to the biosphere sink. Such simulations may also provide a framework for a top-down assessment of our anthropogenic inventory when combined with atmospheric measurements. This top-down assessment would require atmospheric observations for times (e.g., winter) and locations (e.g., western U.S.) in which the industrial source may be dominant and the biosphere sink relatively small. Future field campaigns would be needed to support such an assessment. However, even without a top-down assessment, our updated inventory provides a significant advance over the previous Kettle inventory which was based on a small subset of the published emission factor data and outdated industry activity data.

Acknowledgments
This work was supported by the U.S. Department of Energy, Office of Science, and Office of Terrestrial Ecosystem Sciences. Monthly coal consumption data were provided by K. Gurney. Requests for data used in this paper can be directed to Elliott Campbell (ecampbell3@ucmerced.edu) and are also available at https://eng.ucmerced.edu/campbell/.

References

Apodaca, L. E. (2015), Mineral commodity summaries: Sulfur, *Miner. Inf.*, *703*, 156–157. [Available at https://minerals.usgs.gov/minerals/pubs/commodity/sulfur/.]

Berry, J., et al. (2013), A coupled model of the global cycles of carbonyl sulfide and CO_2: A possible new window on the carbon cycle, *J. Geophys. Res. Biogeosci.*, *118*, 842–852, doi:10.1002/jgrg.20068.

Blagoev, M., and C. Funada (2011), Marketing research report: Carbon disulfide, CEH, (625.5000C), pp. 1–65. [Available at https://www.ihs.com/products/chemical-economics-handbooks.html.]

Blake, N. J., et al. (2004), Carbonyl sulfide and carbon disulfide: Large-scale distributions over the western Pacific and emissions from Asia during TRACE-P, *J. Geophys. Res.*, *109*, D15S05, doi:10.1029/2003JD004259.

Blake, N. J., et al. (2008), Carbonyl sulfide (OCS): Large-scale distributions over North America during INTEX-NA and relationship to CO_2, *J. Geophys. Res.*, *113*, D09S90, doi:10.1029/2007JD009163.

Fiber Economics Bureau (2014), Fiber Organon, pp. 94–116. [Available at http://www.fibereconomics.com/feb3c.htm.]

Campbell, J. E., et al. (2007), Analysis of anthropogenic CO_2 signal in ICARTT using a regional chemical transport model and observed tracers, *Tellus B*, *59*(2), 199–210, doi:10.1111/j.1600-0889.2006.00239.x.

Campbell, J. E., et al. (2008), Photosynthetic control of atmospheric carbonyl sulfide during the growing season, *Science*, *322*(5904), 1085–1088, doi:10.1126/science.1164015.

Campbell, J. E., M. E. Whelan, U. Seibt, S. J. Smith, J. A. Berry, and T. W. Hilton (2015), Atmospheric carbonyl sulfide sources from anthropogenic activity: Implications for carbon cycle constraints, *Geophys. Res. Lett.*, *42*, 3004–3010, doi:10.1002/2015GL063445.

Carmichael, G. R., L. K. Peters, and R. D. Saylor (1991), The STEM-II regional scale acid deposition and photochemical oxidant model—I. An overview of model development and applications, *Atmos. Environ. A.General Top.*, *25*(10), 2077–2090, doi:10.1016/0960-1686(91)90085-L.

Chin, M., and D. D. Davis (1993), Global sources and sinks of OCS and CS_2 and their distributions, *Global Biogeochem. Cycles*, *7*, 321–337, doi:10.1029/93GB00568.

Commane, R., L. K. Meredith, I. T. Baker, J. A. Berry, J. W. Munger, S. A. Montzka, P. H. Templer, S. M. Juice, M. S. Zahniser, and S. C. Wofsy (2015), Seasonal fluxes of carbonyl sulfide in a midlatitude forest, *Proc. Natl. Acad. Sci. U. S. A.*, *112*(46), 14,162–14,167, doi:10.1073/pnas.1504131112.

Cox, P. M., R. A. Betts, C. D. Jones, S. A. Spall, and I. J. Totterdell (2000), Acceleration of global warming due to carbon-cycle feedbacks in a coupled climate model, *Nature*, *408*(6809), 184–187.

D'Allura, A., et al. (2011), Meteorological and air quality forecasting using the WRF–STEM model during the 2008 ARCTAS field campaign, *Atmos. Environ.*, *45*(38), 6901–6910, doi:10.1016/j.atmosenv.2011.02.073.

Field, C. B., D. B. Lobell, H. A. Peters, and N. R. Chiariello (2007), Feedbacks of terrestrial ecosystems to climate change, *Annu. Rev. Environ. Resour.*, *32*(1), 1–29, doi:10.1146/annurev.energy.32.053006.141119.

Friedlingstein, P., et al. (2006), Climate–carbon cycle feedback analysis: Results from the C4MIP model intercomparison, *J. Clim.*, *19*(14), 3337–3353, doi:10.1175/JCLI3800.1.

Friedlingstein, P., M. Meinshausen, V. K. Arora, C. D. Jones, A. Anav, S. K. Liddicoat, and R. Knutti (2014), Uncertainties in CMIP5 climate projections due to carbon cycle feedbacks, *J. Clim.*, *27*(2), 511–526, doi:10.1175/JCLI-D-12-00579.1.

Glatthor, N., et al. (2015), Tropical sources and sinks of carbonyl sulfide observed from space, *Geophys. Res. Lett.*, *42*, 10,082–10,090, doi:10.1002/2015GL066293.

Gurney, K. R., et al. (2002), Towards robust regional estimates of CO_2 sources and sinks using atmospheric transport models, *Nature*, *415*(6872), 626–630, doi:10.1038/415626a.

Hilton, T. W., A. Zumkehr, S. Kulkarni, J. Berry, M. E. Whelan, and J. E. Campbell (2015), Large variability in ecosystem models explains uncertainty in a critical parameter for quantifying GPP with carbonyl sulphide, *Tellus B*, *67*, doi:10.3402/tellusb.v67.26329.

Joint Research Centre (2011), Global emissions EDGAR v4.2. [Available at http://edgar.jrc.ec.europa.eu.]

Kettle, A. J., U. Kuhn, M. von Hobe, J. Kesselmeier, and M. O. Andreae (2002), Global budget of atmospheric carbonyl sulfide: Temporal and spatial variations of the dominant sources and sinks, *J. Geophys. Res.*, *107*(22), 4658, doi:10.1029/2002JD002187.

Kimmerle, F., and L. Noel (1997), *COS, CS_2 and SO_2 Emissions from Prebake Hall Heroult Cells*, pp. 153–158, Arvida Res. Dev. Cent, Orlando, Fla.

Kuai, L., et al. (2015), Estimate of carbonyl sulfide tropical oceanic surface fluxes using Aura Tropospheric Emission Spectrometer observations, *J. Geophys. Res. Atmos.*, *120*, 11,012–11,023, doi:10.1002/2015JD023493.

Kulkarni, S., et al. (2014), Source sector and region contributions to BC and $PM_{2.5}$ in central Asia, *Atmos. Chem. Phys. Discuss.*, *14*(8), 11,343–11,392, doi:10.5194/acpd-14-11343-2014.

Launois, T., P. Peylin, S. Belviso, and B. Poulter (2014), A new model of the global biogeochemical cycle of carbonyl sulfide – Part 2: Use of OCS to constrain gross primary productivity of current vegetation models, *Atmos. Chem. Phys. Discuss.*, *14*(20), 27,663–27,729, doi:10.5194/acpd-14-27663-2014.

Lee, C. L., and P. Brimblecombe (2016), Anthropogenic contributions to global carbonyl sulfide, carbon disulfide and organosulfides fluxes, *Earth Sci. Rev.*, *160*, 1–18, doi:10.1016/j.earscirev.2016.06.005.

Maseyk, K., J. A. Berry, D. Billesbach, J. E. Campbell, M. S. Torn, M. Zahniser, and U. Seibt (2014), Sources and sinks of carbonyl sulfide in an agricultural field in the Southern Great Plains, *Proc. Natl. Acad. Sci. U. S. A.*, *111*(25), 9064–9069, doi:10.1073/pnas.1319132111.

Montzka, S. A., P. Calvert, B. D. Hall, J. W. Elkins, T. J. Conway, P. P. Tans, and C. Sweeney (2007), On the global distribution, seasonality, and budget of atmospheric carbonyl sulfide (COS) and some similarities to CO_2, *J. Geophys. Res.*, *112*, D09302, doi:10.1029/2006JD007665.

Peyton, T. O., R. V. Steele, and W. R. Mabey (1978), *Carbon Disulfide, Carbonyl Sulfide: Literature Review and Environmental Assessment*, Environ. Protection Agency, Office of Health and Ecol. Effects, Washington, D. C.

Pos, W. H., and H. Berresheim (1993), Automotive tire wear as a source for atmospheric OCS and CS_2, *Geophys. Res. Lett.*, *20*, 815–817, doi:10.1029/93GL00972.

Sandoval-Soto, L., M. Stanimirov, M. von Hobe, V. Schmitt, J. Valdes, A. Wild, and J. Kesselmeier (2005), Global uptake of carbonyl sulfide (COS) by terrestrial vegetation: Estimates corrected by deposition velocities normalized to the uptake of carbon dioxide (CO_2), *Biogeosciences*, *2*(2), 125–132.

Stimler, K., S. A. Montzka, J. A. Berry, Y. Rudich, and D. Yakimir (2010), Relationships between carbonyl sulfide (COS) and CO_2 during leaf gas exchange, *New Phytol. Trust*, *186*(4), 869–878.

U.S. Energy Information Administration (2002), *Annual Energy Review*, U.S. Department of Energy, Washington, D. C.

U.S. Energy Information Administration (2003), *Annual Energy Review 2002*, U.S. Department of Energy, Washington, D. C.

U.S. Geological Survey (2013), 2012 minerals yearbook: Aluminum. [Available at https://minerals.usgs.gov/minerals/pubs/commodity/aluminum/myb1-2012-alumi.pdf.]

Utne, I., K. A. Paulsen, and J. Thonstad (1998), The emission of carbonyl sulphide from prebake and Söderberg aluminium cells, in *Light Metals*, pp. 293–301, TMS, Orlando, Fla.

Wang, Y., et al. (2016), Towards understanding the variability in biospheric CO_2 fluxes: Using FTIR spectrometry and a chemical transport model to investigate the sources and sinks of carbonyl sulfide and its link to CO_2, *Atmos. Chem. Phys.*, *16*(4), 2123–2138, doi:10.5194/acp-16-2123-2016.

Whelan, M. E., T. W. Hilton, J. A. Berry, M. Berkelhammer, A. R. Desai, and J. E. Campbell (2016), Carbonyl sulfide exchange in soils for better estimates of ecosystem carbon uptake, *Atmos. Chem. Phys.*, *16*(6), 3711–3726, doi:10.5194/acp-16-3711-2016.

Zumkehr, A., and J. E. Campbell (2013), Historical U.S. cropland areas and the potential for bioenergy production on abandoned croplands, *Environ. Sci. Technol.*, *47*(8), 3840–3847.